DRUG DEVELOPMENT AND INDUSTRIAL PHARMACY, 9(8), 1417-1434 (1983)

PHYSICAL ASPECTS OF WET GRANULATION III. EFFECT OF WET GRANULATION ON GRANULE POROSITY

M.A. Zoglio*, and J.T. Carstensen**

Merrell Research Center, Merrell Dow Pharmaceuticals Inc., Subsidiary of The Dow Chemical Company, Cincinnati, Ohio 45215, and
**School of Pharmacy, University of Wisconsin, Madison, Wisconsin 53706.

ABSTRACT

The porosity of granules produced by wet granulation has been studied using mercury porosimetry. Granule pore size distribution appears to be bimodal, with a population of micropores and macropores. Pore surface area varies with kneading time, going through a maxima at a point where physical properties such as flow and bulk density also exhibit a maxima. True granule density displays a direct relationship to rate of flow. The information in general supports the postulate that equilibrium microporous granules are formed first in the wet granulation process, followed by consolidation with subsequent formation of macroporous twins and agglomerates.

* To whom correspondence should be directed.

 0363-9045/83/0908-1417$3.50/0

INTRODUCTION

The pore structure of granules is important in terms of *in vitro* disintegration (1) and dissolution (2).

Mercury porosimetry has been used in this study to elucidate granule pore characteristics. Similar studies have been reported for powders (3-6). The powder data does not relate well to the findings for granules. For example, the pore size distribution for prime powder particles follows a single log probit function. The distribution for the granules in this report (7,8) is at least bimodal with neither population being log probit in nature. The intent of the present investigation is to examine granule porosity measurements for correlation with other important physical properties and to gain insight into the mechanism of granule formation for the system studied (7,8).

EXPERIMENTAL

A wet granulation was prepared in a chopper-ribbon blender. [1] The formula was the one previously reported by Zoglio et al. (7) and Carstensen et al. (8) and is repeated here for convenience: 18 Kg of lactose U.S.P., 10.7 Kg of sucrose U.S.P., and 4.35 Kg of cornstarch U.S.P. were mixed for 5 minutes in the mixer. 0.15 Kg of cornstarch dissolved in 3 liters of water were then added, and mixing continued for various times (1, 3, 5, 10, 15, and 20 minutes). The granulation was dried in a fluid bed dryer [2] at 42°C, with an air velocity of 380 cubic feet per minute to an exit temperature of 35°C.

---

[1] Model FM-100 Littleford-Lodige, Cincinnati, Ohio

[2] Aeromatic A.G., Basel, Switzerland

The granulation thus formed was sieved and the sieve fractions were subjected to mercury porosimetry.[3]

RESULTS AND DISCUSSION

Pore Size

The average pore diameter for each sieve fraction is listed in Table I.

It is shown in the last line of Table I that there is a distinct demarcation in mean pore size for the smaller fraction, i.e., those granules smaller than 60 mesh and those above. The former have mean pore sizes of 0.1 - 0.14 μm, and the latter have pore sizes of 0.23 - 0.26 μm.

The smaller mean pore size is probably due to the formation of smaller granules primarily from prime powder particles, whereas the larger value results from twinning and agglomeration of smaller granules to form larger granules. As seen from the last column, the time of kneading does not affect the mean pore diameter, presumably because compaction of porous granules (which would reduce the mean pore diameter) is offset by twinning and agglomeration (increasing the mean pore diameter).

Pore Size Distribution

The pore size distribution shown in Figure 1 has at least two distinct modes with a break point at about 0.5 μm. Weibull plotting of the data from Table IIA indicates the breakoff point or lower pore size limit for the macropores to be 0.543 μm. The linearity of the Weibull distribution function for the macropores using

[3] Micromeritics Instrument Corporation, 5680 Goshen Springs Road, Norcross, Georgia, 30093

TABLE I

Average Pore Diameter [4V/A(μm)]

Time Min.	80/Pan	60/80	40/60	20/40	14/20	10/14	$\bar{x}$	$\frac{S}{x}$
1	0.19	0.22	0.15	(0.91)*	(0.88)*	0.20	0.19	0.015
3	0.14	0.20	0.10	0.33	0.28	0.27	0.22	0.036
5	0.10	0.13	0.08	0.17	0.20	0.23	0.15	0.024
10	0.07	0.09	0.10	0.16	0.23	0.38	0.17	0.050
15	0.12	0.12	0.12	0.27	0.22	0.27	0.19	0.031
20	0.11	0.11	0.09	0.38	(0.54)*	0.22	0.17	0.058
$\bar{x}$	0.121	0.142	0.103	0.263 (0.370)*	0.233 (0.392)*	0.262		
$S_{\bar{x}}$	0.017	0.023	0.012	0.043 (0.114)*	0.017 (0.110)*	0.026		

* Outliers have been omitted in the averages not in parenthesis.

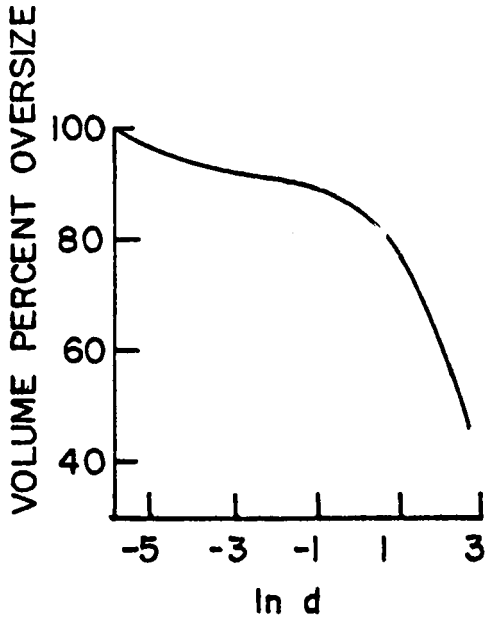

Fig. 1 - Pore size distribution of 20/40 mesh cut from granulation kneaded for one minute.

the 0.543 μm break point is shown in Figure 2. Plotting of the macropore data for normal and log normal distribution gave poor results.

The micropore data listed in Table IIB is plotted in Figure 3 for Weibull and log normal functions. The micropore distribution is poorly described by Figure 3 and also by the normal distribution function.

The evidence for two distinct populations of pores gives credence to the postulate (7, 8) that granule building involves formation initially of microporous equilibrium granules from prime powders. These granules then consolidate, twin, and agglomerate to form larger macroporous granules.

Pore Volume

The initially high pore volume, (Table III, and Figure 4) reflects the microporosity of the primary

TABLE IIA

Macropore Size Distribution

Diameter d (μm)	Pore Volume* cc/g >d	Macro Fraction >d	Weibull Parameter	
21.487	0.0740	1-y	ln(-ln(1-y))	ln d
17.145	0.0914	0.11	0.60	2.84
13.9011	0.1076	0.21	0.45	1.63
11.299	0.1223	0.30	0.19	2.42
9.0533	0.1359	0.39	-0.05	2.20
7.2634	0.1469	0.45	-0.24	1.98
6.3142	0.1486	0.46	-0.27	1.84
4.6758	0.1626	0.55	-0.52	1.54
3.7237	0.1758	0.63	-0.79	1.31
3.0479	0.1894	0.72	-1.11	1.11
2.4157	0.2045	0.81	-1.57	0.88
1.3021	0.2242	0.94	-2.70	0.26
0.8229	0.2304	----	-----	-0.19
0.5430	0.2346	1.00	-----	----

* The total pore volume is 0.2489 cc/g. In Fig. 1 the data in this column are shown on a percentage basis, e.g., for d = 11.3, the percentage is 0.1223/0.2489 = 49%.

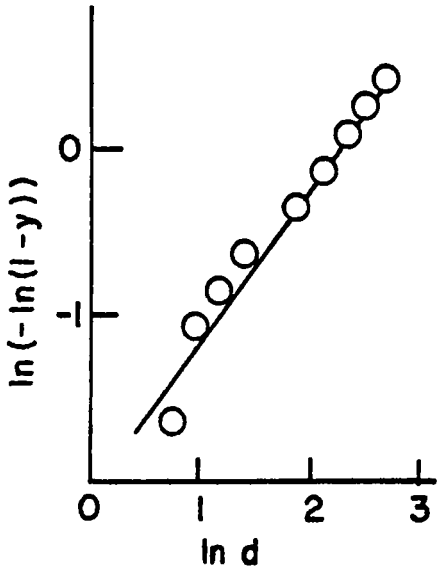

Fig. 2 - Macropore distribution of granule pore size above 0.54 μm from Fig. 1 (Table IIA) presented as a Weibull function.

granules. Dissolution of matrix components of the microporous granules causes consolidation and decreases pore volume. Following the shallow minima of Figure 4, twinning and agglomeration causes macroporosity so that the overall pore volume/porosity per gram increases slightly.

The pore volumes (cc/g) have been converted to porosity (dimensionless) (Table III) for each sieve fraction. The granule density ρ_p in g/cc as determined by mercury porosimetry is used to calculate porosity. The data are plotted in Figure 5.

It is noted that

$$\ln_{\varepsilon} = a \ln D + b \qquad \text{(Eq. 1)}$$

where ε is the porosity, D is the granule diameter and the least squares fit values of the constants a and b are a = 0.344 and b = 3.11 (R = 0.84). The format in

TABLE IIB

Micropore Size Distribution

Diameter d (μm)	Pore Volume* cc/g >d	Micro Fraction >d	Weibull Parameter	
0.5430	0.2346	1-y	ln(-ln(1-y))	ln d
0.4257	0.2358	0.084	0.91	-0.85
0.3480	0.2367	0.15	0.64	-1.06
0.2836	0.2371	0.18	0.53	-1.26
0.2251	0.2380	0.24	0.36	-1.49
0.0772	0.2392	0.32	0.13	-2.56
0.0262	0.2400	0.37	-0.026	-3.64
0.0111	0.2416	0.49	-0.34	-4.50
0.0071	0.2429	0.58	-0.61	-4.95
0.0058	0.2437	0.64	-0.79	-5.15
0.0047	0.2456	0.77	-1.34	-5.36
0.0038	0.2467	0.85	-1.79	-5.58
------	0.2489	----	-----	-----

* In Fig. 1, this is shown on a percentage basis, e.g., for d = 0.026, the percentage is 100 0.24/0.2489 = 96.4%.

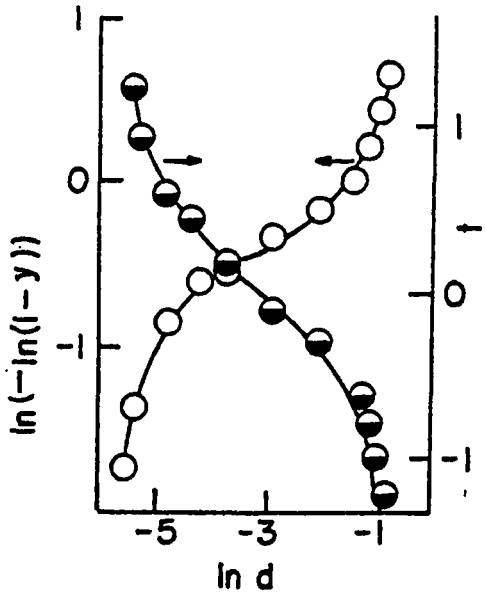

Fig. 3 - Micropore distribution of granule pore size below 0.54 μm from Fig. 1 (Table IIB) presented as a Weibull function. (○) and as a log-normal distribution (◒).

Eq. 1, of course, is approximate, since ε cannot surpass unity.

Pore Surface Area

Pore surface area values for each mesh cut are listed in Table IV. Similar to pore volume, the specific area of pores increases with increasing granule size. Once again, the twinning and aggregation effect producing the larger granules yields higher porosity. The sieve analysis data in Table IV is used to calculate area in meters squared per gram for the total granulation system at different kneading times.

A_i denotes pore surface area per grams of sieve cut_i and P_i denotes the weight percent of sieve cut_i.

TABLE III

Pore Volume (cc/g) As a Function of Sieve Fraction and Kneading Time

Time (Min)	80/Pan (88 μm)	60/80 (214 μm)	40/60 (335 μm)	20/40 (630 μm)	14/20 (1190 μm)	10/14 (1770 μm)	% of 1 Minute Figure 80/Pan	60/80	40/60	20/40	14/20	10/14	$\bar{x}$	$S_{\bar{x}}$
1	0.32	0.34	0.39	0.62	1.16	1.07	100	100	100	100	100	100	100	0
3	0.25	0.24	0.27	0.60	0.90	0.97	78	71	69	97	78	91	81	4.5
5	0.20	0.18	0.24	0.55	0.64	0.90	63	53	62	89	55	84	68	6.2
10	0.15	0.14	0.14	0.35	0.78	0.88	47	41	36	56	67	82	55	7.0
15	0.11	0.17	0.20	0.48	0.99	0.93	34	50	51	77	85	87	60	9.0
20	0.16	0.16	0.20	0.44	0.92	0.97	50	48	51	71	79	91	53	13.0
$\bar{x}$	0.098	0.205	0.240	0.507	0.898	0.953								
$\ln \bar{x}$	-1.63	-1.58	-1.43	-0.68	-0.11	-0.05								
$S_{\bar{x}}$	0.031	0.030	0.035	0.402	0.073	0.028								
ρ_p	1.29	1.19	1.13	0.86	0.65	0.62								
ϵ^*	0.13	0.24	0.27	0.44	0.58	0.59								
$\ln\epsilon$	-2.04	-1.44	-1.32	-0.83	-0.55	-0.52								
$\ln D_1$	4.48	5.37	5.81	6.45	7.08	7.48								

*Conversion from cc/g to dimensionless quantity is based on the particle density of the solids as determined by mercury porosimetry of the solids.

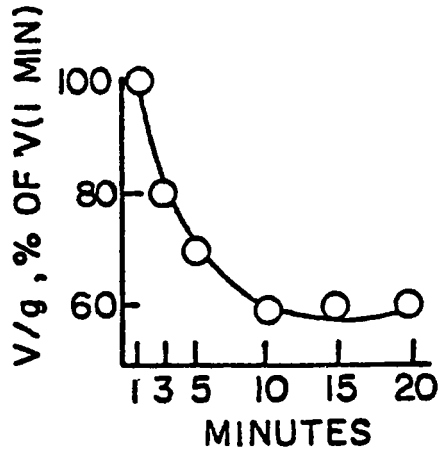

Fig. 4 - Total pore volume (cc/g) as a function of kneading time (Table III).

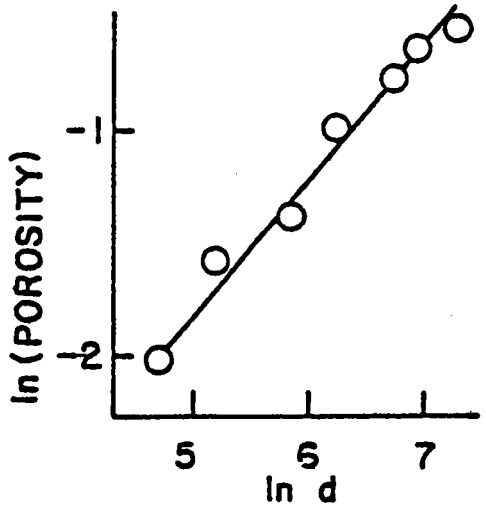

Fig. 5 - Porosity (Table III) as a function of granule size (diameter) D_i (Table III) (in μm).

TABLE IV

Pore Surface Areas, m^2/g of Various Mesh Cuts at Various Kneading Times, t Minutes, Weight Percent, p_i, of Mesh Cut, and Total Pore Surface Area, A $m^2/100$ g of Granulation.

t Min	80/Pan (88 μm) m^2/g	p_i%	60/80 (215 μm) m^2/g	p_i%	40/60 (335 μm) m^2/g	p_i%	20/40 (630 μm) m^2/g	p_i%	14/20 (1190 μm) m^2/g	p_i%	10/14 (1770 μm) m^2/g	p_i%	A m^2 Per 100 g	Average Granule Diameter (D)
1	6.82	34	6.04	11	10.86	12	2.74	14	5.25	15	20.97	14	839	608
3	7.00	8	4.80	13	11.18	42	7.20	20	13.06	10	14.35	7	963	540
5	8.10	4	5.34	7	12.57	36	12.62	35	12.82	13	15.82	5	1210	603
10	8.56	1.1	6.68	1.5	5.65	11	8.86	28	13.62	47.4	9.31	11	1078	976
15	3.55	6	5.91	5	6.82	14	7.11	30	1.77	28	14.01	17	647	890
20	5.96	5	7.04	4.5	0.12	12	4.70	29	6.82	29	17.40	20.5	754	945
Mean	6.67		5.97		7.87		8.09		8.89		15.31			
SEM*	0.73		0.34		1.89		1.31		2.02		1.58			

* Standard Error of the Mean

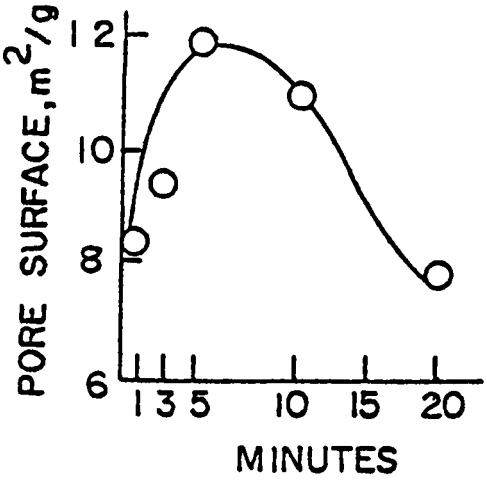

Fig. 6 - Specific pore surface area (Table IV) as a function of kneading time.

The pore surface A per 100 g of granulation for the six fractions is:

$$A = \sum_{i=1}^{6} A_i P_i \qquad \text{(Eq. 2)}$$

A most interesting finding is the maximum in surface area at 5-10 minutes kneading time (Figure 6). The optimum in physical properties such as flow and bulk density is also found at 5-10 minutes kneading time (Tables V and VI). This is in line with previous findings (9) for this specific granulation. The existence of a maximum in granule properties at characteristic kneading times indicates the possibility that meaningful granulation end points can be found through assessment of granule properties at various kneading times.

Granule Density

Granule density, as determined by mercury porosimetry, is defined as the density of the individual granules excluding void space between granules, i.e.,

TABLE V

Flow Rates (g/sec) as a Function of Granule Size and Kneading Time

Kneading Time, Min.	80/Pan (88 μm)	60/80 Mesh (215 μm)	40/60 Mesh (335 μm)	20/40 Mesh (630 μm)	14/20 Mesh (1190 μm)	Avg. of Row	Standard Error
1	3.42	3.50	3.60	3.74	2.98	3.44	0.33
3	3.70	3.76	4.28	4.43	3.70	3.91	0.19
5	IS*	5.05	5.01	4.95	3.82	4.71	0.3
10	IS*	IS*	5.18	5.04	4.56	4.98	0.2
15	IS*	IS*	4.96	4.28	3.38	4.21	0.5
20	IS*	IS*	4.85	4.49	3.74	4.36	0.3
$\bar{W}$	3.56	4.10	4.65	4.48	3.96		
Std. Error	0.14	0.5	0.2	0.2	0.2		
ρ_p	1.31	1.14	1.095	0.84	0.63		
$\ln(\frac{W}{\rho_p})$	1.16	1.31	1.38	1.65	1.74		
$\ln(D)$	4.48	5.37	5.81	6.45	7.08		

TABLE VI

Apparent Densities (g/cm^3) as a Function of Kneading Time and Granule Size

Time, Min.	80/pan (88 μm)	60/80 Mesh (215 μm)	40/60 Mesh (335 μm)	20/40 Mesh (630 μm)	14/20 Mesh (1190 μm)	Average Apparent Density, ρ^1	Standard Error
1	0.54	0.54	0.55	0.54	0.55	0.543	0.002
3	0.58	0.54	0.56	0.61	0.59	0.576	0.01
5	IS*	0.59	0.61	0.65	0.65	0.625	0.015
10	IS*	IS*	0.65	0.69	0.72	0.687	0.02
15	IS*	IS*	0.59	0.62	0.63	0.613	0.012
20	IS*	IS*	0.60	0.64	0.66	0.633	0.017

*IS = Insufficient Sample

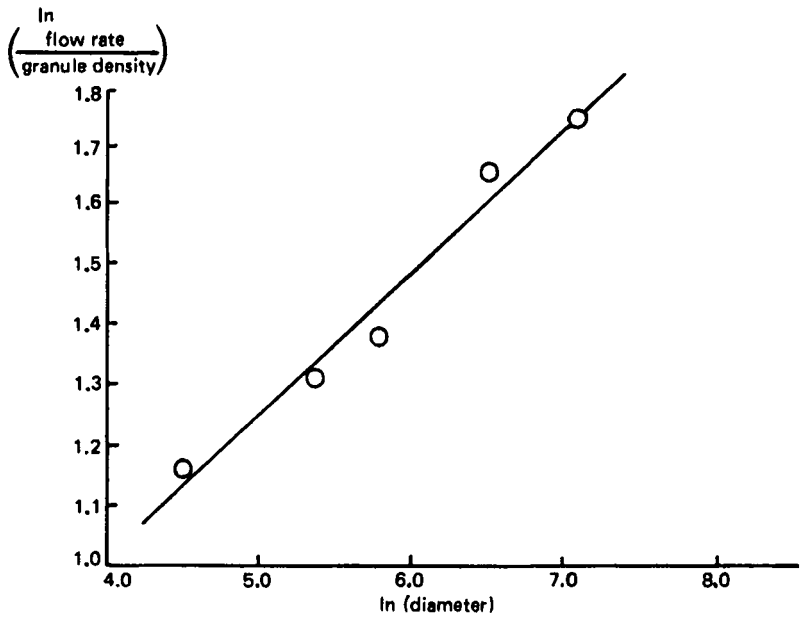

Fig. 7 - Ln of the ratio of flow rate to granule density $(\frac{W}{\rho_p})$ as a function of ln diameter (D) (Table V).

the smaller the granule density the higher the volume of pore space within that granule.

Granule density ρ_p for each sieve fraction is listed in Table V. The granule density decreases with increasing size as would be expected from the pore volume and pore surface data.

There is a relationship between the granule density (ρ_p), granule diameter (D), and flow rate (W), Figure 7 (from values in Table V) such that

$$\ln\left(\frac{W}{\rho_p}\right) = .24 \ln(D) + 0.64 \quad (r^2 = .96) \qquad \text{(Eq. 3)}$$

A controversy exists in the literature as to whether the flow rate (W) is proportional to the granule

density (10) or the bulk density (11). The data reported here favors the former view since equation 3 may be written*

$$W = 1.07\ \rho_p \cdot D^{0.24} \qquad \text{(Eq. 4)}$$

* D here is granule diameter and not orifice diameter. The latter has been kept constant in this study (0.63 cm).

ACKNOWLEDGEMENTS

The authors are indebted to Mr. Kenneth A. Adams for valuable assistance in the experimental portion of the work.

REFERENCES

(1) P. Couvreur, Ph.D. Thesis, Universite Catholique de Louvaine, Brussels, Belgium (1975).

(2) Odile Cruaud, D. Duchene, F. Puisieux, and J.T. Carstensen, J. Pharm. Sci., 69, 608 (1980).

(3) K. Marshall and D. Sixsmith, Drug. Dev. Commun., 1, 51 (1974/75).

(4) L. VanCampen, G. Zografi and J.T. Carstensen, Int. J. Pharmaceu., 5, 1 (1980).

(5) M. Schwarts, J. Pharm. Sci., 63, 774 (1974).

(6) J.T. Carstensen, P. Tovre, L. VanCampen, and G. Zografi, J. Pharm. Sci., 69, 742 (1980).

(7) M.A. Zoglio, H.E. Huber, G. Koehne, P. Chan, and J.T. Carstensen, J. Pharm. Sci., 65, 1205 (1976).

(8) J.T. Carstensen, T. Lai, D.W. Flickner, H.E. Huber and M.A. Zoglio, J. Pharm. Sci., 65, 992 (1976).

(9) J.T. Carstensen and P.C. Chan, J. Pharm. Sci., 66. 1235 (1977).

(10) I.R. McDougall and A.C. Evans, Rheol. Acta, 4, 218 (1965).

(11) T.M. Jones and N. Pilpel, J. Pharm. Pharmacol., 18, 81 (1966a).